



ORR PERFORMANCE OF Pt-OXIDE-C ELECTROCATALYSTS PREPARED BY CVD

Beatriz Ruiz Camacho^{1,*}, Arturo Patiño Rojas¹, Rosa Guadalupe González Huerta¹, Miguel A. Valenzuela¹, Roberto Vargas García², Nicolás Alonso-Vante³.

¹IPN-ESIQIE, Lab. Catálisis y Materiales, CP. 07738, México D.F.

²IPN, ESQIE, Depto. Ing. Metalúrgica, CP. 07738, México D.F.

³LACCO, CNRS-UMR6503, University of Poitiers, Poitiers 86022, France

*contact email: beatrizruizcamacho@gmail.com

ABSTRACT

Low durability of Pt/C electrocatalysts in the polymer electrolyte membrane fuel cells (PEMFC) caused by, e.g., carbon oxidation to CO₂ in acid medium has been recognized as one of the most important drawbacks for long term stability. The additions of different semiconductor oxides, such as TiO₂, SnO₂ or WO₃, confer stability to metal center on carbon-composites, and improve PEMFC performance. In this work, a series of 10%Pt-C and 10%Pt-5%oxide-carbon composites using three oxides (TiO₂, SnO₂, ZnO) has been prepared by a chemical vapor deposition method (CVD). The physical and electrochemical properties were investigated by XRD, hydrogen chemisorption, TEM, CO stripping, cyclic and linear voltammetry as characterization techniques. The prepared materials were electrochemically evaluated in the oxygen reduction reaction (ORR) in acid medium at room temperature. XRD results show a Pt crystalline structure in the different materials synthesized. The average particle size of Pt was determined by hydrogen chemisorption. The size and morphology of Pt nanoparticles were confirmed by TEM. 10%Pt-5%TiO₂-C electrocatalyst showed the higher electrochemical active surface area and the better activity results for the ORR compared with 10%Pt-C, 10%Pt-5%SnO₂-C and 10%Pt-5%ZnO-C materials.

Key words: Electrocatalysts, Pt-oxide-C, CVD, Platinum, ORR.



1. INTRODUCTION

Research and development of Polymer Electrolyte Membrane Fuel Cells (PEMFC) has been devoted to produce a commercially viable product [1]. Among all components of a single membrane electrode assembly (MEA) it is estimated that the polymer electrolyte membrane and precious metal cost contribute to more than 80% of the MEA cost [2]. The most widely used cathode catalyst system for the oxygen reduction reaction (ORR) is platinum particles (range 2-5 nm) dispersed on an electron-conducting support material, typically carbon black (Vulcan XC-72 with 20-30 nm diameter in size) [3]. Supported catalysts have resulted in a 10-100 fold increase in Pt surface area compared to the unsupported platinum used in the early PEMFC systems [4]. Indeed, the shape of nanocrystals plays an important role in the performance of an electrocatalyst, mainly in the adsorption of species involved in the electrochemical reaction [5]. It has been reported that Pt multioctahedrons are more active and stable than the commercial Pt/C (E-TEK) due to the high ratio of (111) to (100) as exposed facets [6].

The stability of electrocatalysts and low durability has recently been recognized as one of the most important issues to be addressed before PEMFC become commercially viable. The degradation of Pt/C catalysts over time is mainly attributed to the loss of electrochemical surface area due the corrosion and electro-oxidation carbon leading to significant electrochemical activity loss [7-8]. One alternative for increase the stability of the electrocatalysts is the use of more stable carbon support. One of the emerging candidates as resistant catalysts supports are the conducting oxides as TiO_2 [9-14], WO_3 [11,15], SnO_2 [16-17] and NbO_2 [17] to produce stables oxide-carbon nanocomposites as Pt substrates. These novel Pt-metal oxide-C electrocatalysts have proved to increase the catalytic activity and stability for Oxygen Reduction Reaction (ORR). For instance, the Pt/ TiO_2 /C composite presented a higher electrocatalytic current per unite area that a conventional Pt/C [9-21]. This behavior was explained in terms of the synergetic effect of the interaction metal-oxide, the presence of oxide produced modifications in the electronic properties of Pt surface, that increase the electronic density of the Pt orbital, these changes are favorable for the adsorption of oxygen and electrochemical activity, suggesting that

Pt–TiO₂–C might serve as stable catalysts of response to lower the amount of utilized platinum in low temperature H₂/O₂ fuel cells cathodes [11, 22].

The preparation of catalysts is a fundamental step to obtain the desired activity, selectivity and life time [23]. Several methods of synthesis had been probed to increase the activity of the conventional electrocatalyst Pt-C in a PEMFC. In order to improve the advantages obtained in the last researches, in this work we probe a new methodology as alternative method (chemical vapor deposition technique) to prepare actives and stable electrocatalysts for PEMFC. Is reported that the use of this technique produced well dispersed nanoparticles ranging from 1-20 nm depending on their chemical nature and the deposition conditions have been obtained under different powdered substrates [24].

In the present research we developed an experimental procedure to obtain and characterize 10%Pt-5%oxide-C (TiO₂, SnO₂, ZnO) electrocatalysts prepared by chemical vapor deposition method. 10%Pt-C electrocatalysts was prepared by the same methods as comparative purposes. The physical and electrochemical properties of the solids were studied by XRD, TEM, H₂ chemisorption and CO stripping techniques. The electrochemical activity was evaluated in the ORR in sulfuric acid at room temperature.

2. EXPERIMENTAL

2.1. Materials

Platinum acetyl acetonate [(CH₃-COCHCO-CH₃)₂Pt] (Aldrich), Carbon (Vulcan XC-72), TiO₂ rutile, SnO₂ and ZnO nanoparticles (Aldrich) were the precursors for the Pt-oxide-C nanocomposites preparation.

2.2. Pt-C and Pt-oxide-C preparation by chemical vapor deposition

A thermal horizontal tube quartz reactor were used for the chemical vapor deposition (CVD) method (see Fig. 1). The syntesis of Pt-C was carried out using platinum acetylacetonate as metallic precursor in a 10:90 weight ratio Pt:C. The Pt precursor and C were mixed into the

reactor at room temperature, then the system was heated at 200 °C for 10 min using a total pressure of 4.5 torr to carried out a thermal evaporation of platinum precursor. After that, the vapor-impregnated Pt nanoparticles were heated at 250 °C inside the tube reactor to achieve the precursor decomposition. This method allows the formation of Pt nanoparticles uniformly dispersed over carbon.

Table 1. Code and characteristics of Pt/C and Pt/oxide/C electrocatalysts synthesized by chemical vapor deposition.

	Catalysts	Average Particle size of Pt, QH ₂ (nm)	EAS (CO) (cm ²)	Pt dispersion, QH ₂ (%)
(M1)	10%Pt-5%TiO ₂ -C	2.75	4.1	41.08
(M2)	10%Pt-5%SnO ₂ -C	2.6	0.21	43.65
(M3)	10%Pt-5%ZnO-C	2.0	1.62	58.19
(M4)	10%Pt-C	2.3	0.87	33.96

The preparation of 10%Pt-5%oxide-C was carried out using the same conditions above mentioned by mixing the platinum precursor, oxide nanoparticles (TiO₂, SnO₂, ZnO) and carbon Vulcan in 10:5:85 weight ratio, respectively. Table 1 shows the code and clasification of Pt-C and Pt-oxide-C electrocatalysts prepared by chemical vapor deposition (CVD) method.

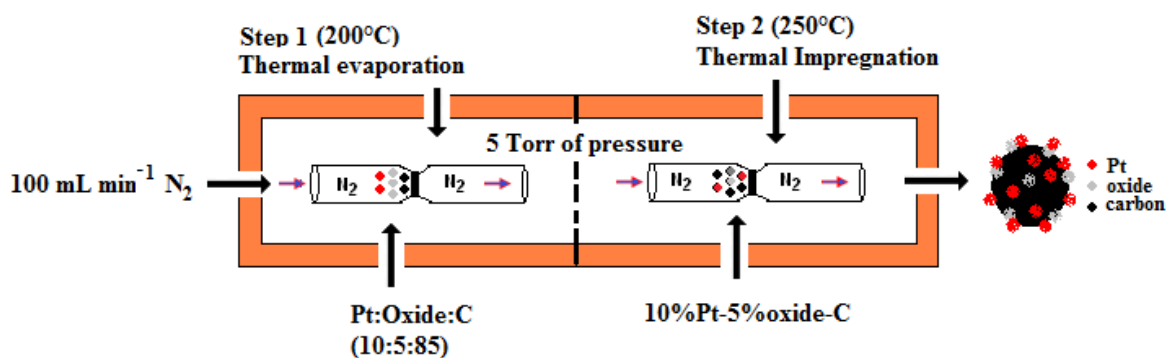


Figure 1. Scheme of Pt-C and Pt-oxide-C catalysts preparation by CVD

2.3. Characterization techniques

X-ray diffraction (XRD) patterns were collected on a Bruker D8 AXS equipment using a Cu anode (K_{α} , $\lambda=1.5406 \text{ \AA}$) and a Bragg-Brentano configuration. The angle 2θ was varied from 30 to 90° with $0.2^{\circ} \text{ min}^{-1}$ and 35 kV . Particle size distribution was obtained with a high resolution transmission electron microscopy using a JEOL-JEM-2200 field emission operated at 200 kV . The H_2 chemisorption (pulse method) test was performed using an Autochem II 2920 equipment (Micromeritics) with a thermal conductivity detector (TCD) to determine the average active particle size and metal dispersion (defined as the number of Pt surface atoms/number of total Pt atoms).

2.4. Electrochemical measurement

All electrochemical measurements were carried out at 25°C in conventional single three-electrode test electrochemical cell. A platinum mesh was used as the counter electrode and $\text{Hg}/\text{Hg}_2\text{SO}_4/0.5\text{M H}_2\text{SO}_4$ ($\text{MSE} = 0.680 \text{ V/NHE}$) as the reference electrode. The potentials in this paper were related to a normal hydrogen electrode (NHE) in a $0.5\text{M H}_2\text{SO}_4$ aqueous solution electrolyte. The rotating disk electrode (RDE) measurements were performed using a Potentiostat (EG&G PAR 263A) and a Pine MSR-X rotation speed controller. Glassy carbon disk with a cross-sectional area of 0.19 cm^2 was used as a support for the thin films and used as an ink-type working electrode. The catalytic ink was prepared with 1mg of catalyst, $6 \mu\text{l}$ of 5 wt\% solution Nafion® (Du Pont, 1100 EW) and $60 \mu\text{l}$ of ethyl alcohol, $8 \mu\text{l}$ of this sonicated mixture were deposited on the working electrode. The estimated amount of Pt-C and Pt-TiO₂-C catalyst on the glassy carbon electrode surface was about 0.63 mg cm^{-2} .

Before the ORR measurements, cyclic voltammetry (CV), in nitrogen-saturated electrolyte, was performed to clean the electrode surface from 0.0 to 1.2 V at 50 mV s^{-1} , 40 cycles were necessary to stabilize the current–potential signal. Thereafter, the acid electrolyte was saturated with pure oxygen and maintained on the electrolyte surface during the RDE tests. Hydrodynamic experiments were recorded in the rotation rate range of 100 to 1600 rpm at 5 mV s^{-1} . Between

RDE measurements, the acid electrolyte was saturated with pure oxygen for 5 min to obtain a stable open circuit potential. The current density was calculated using the geometric surface area.

The experimental technique selected to determinate the Electrochemical Active Surface Area (EAS_{CO}) was the CO stripping technique, using the same quantity of sample, the electrode potential was held at 0.1 V/NHE and CO bubbled for 5 min. Thereafter, the CO was removed by purging the electrolyte with argon during 15 min. Two cycles were done from 0.05 V to 1.2 V/NHE at 5 mV s^{-1} to quantify the area under the curve [25].

3. RESULTS

3.1 X-ray Diffraction

Figure 2 shows the X-ray diffraction patterns of 10%Pt-C and 10%Pt-5%oxide-C catalysts prepared by chemical vapor deposition. In the materials prepared are identified the face-centered cubic (fcc) structure of platinum. The diffraction peaks of Pt were found at $39.8, 46.2, 67.5, 81.3^\circ$ ascribed to the (111), (200), (222) and (311). The Pt-ZnO-C (M3) shows the lower intensity of these peaks. The other diffraction peaks in the samples M1, M2 and M3 can be attributed to the presence of TiO_2 (anatase phase), SnO_2 (casiterite phase) and ZnO, respectively. There is not a shift in any of the crystallographic planes of platinum, indicating not Pt-oxide alloys.

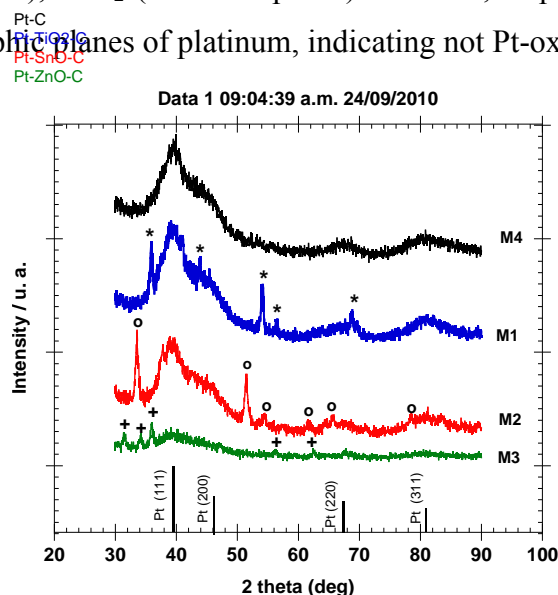


Figure 2. X ray diffraction patterns of (M1)10%Pt-5% TiO_2 -C, (M2)10%Pt-5% SnO_2 -C, (M3)10%Pt-5% ZnO -C and (M4)10%Pt-C electrocatalysts prepared by CVD.

3.2 TEM micrographs

Figure 3 shows TEM images of the Pt-C and Pt-TiO₂-C catalysts. It can be observed that both materials had a similar morphology with uniform distribution on the carbon support. The mean particle size is between 2-4 nm with a spherical or globular morphology.

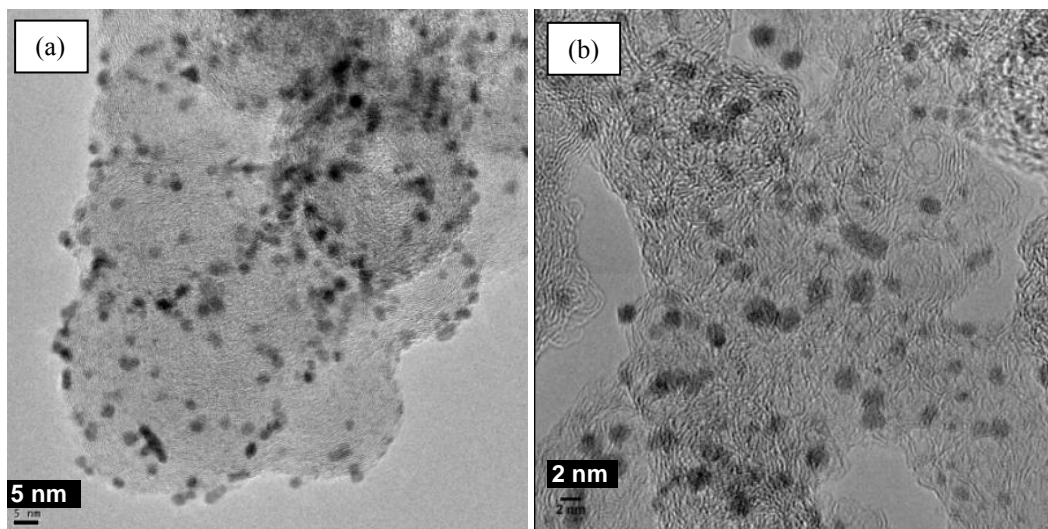


Figure 3. TEM graphs for a) 10%Pt-5%TiO₂-C and b) 10%PtC electrocatalysts synthesized by CVD.

3.3 H₂ Chemisorption

The average diameter of Pt nanoparticles and metal dispersion of Pt-oxide-C and Pt-C samples prepared by chemical vapor deposition method was determined by H₂ chemisorption, results were reported in Table 1. Assuming spherical Pt nanoparticles, the samples Pt-oxide-C prepared by chemical vapor deposition delivered the lower diameter of Pt particle (<3 nm) with the maximum metal dispersion of 40-60% compared with the Pt-C catalysts prepared by the same method. These H₂ chemisorption results agree with the TEM images results.

3.4 CO stripping

Fig. 4 left shows the corresponding cyclic voltammograms (CVs) curves in nitrogen purged 0.5 M H₂SO₄ solution at 25 °C on the Pt-C and Pt-oxide-C electrocatalysts prepared by chemical vapor deposition. The voltammograms curves of Pt-C and Pt-oxide-C electrocatalysts show the

typical characteristics of Pt nanoparticles. Between 0.05 and 0.3 V/NHE hydrogen adsorption-desorption is observed. On the anodic sweep above 0.8 V/NHE, oxide film is formed on the surface of the platinum materials. The oxide film is removed during the cathodic sweep by the oxide reduction, between 0.3-0.6 V/NHE the double layer region is located, which differed on the Pt-TiO₂-C sample due to the TiO₂ presence.

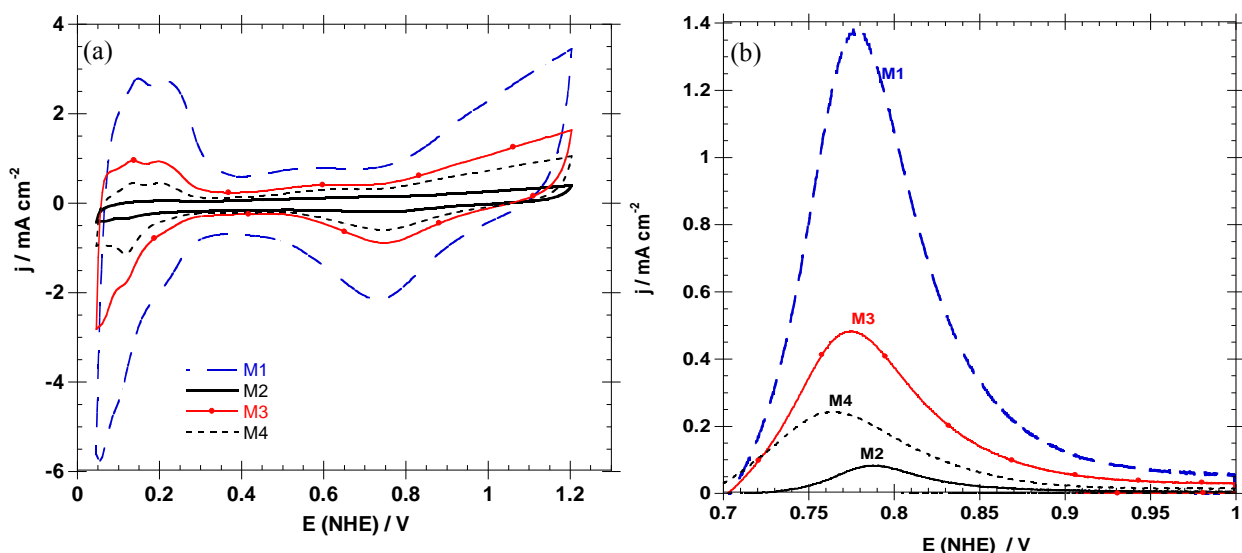


Figure 4. Cyclic voltammograms (50 mV s⁻¹) and CO stripping (5 mV s⁻¹) of (M1) 10%Pt-5%TiO₂-C, (M2) 10%Pt-5%SnO₂-C, (M3) 10%Pt-5%ZnO-C and (M4) 10%Pt-C electrocatalysts in H₂SO₄ 0.5 M at T = 25°C.

The Pt-TiO₂-C and Pt-ZnO-C electrocatalysts presented a better definition of hydrogen adsorption-desorption peaks compared with Pt-SnO₂-C and Pt-C samples. This changes on the hydrogen adsorption-desorption is related with the sized and the crystallographic faces, also depend of the Pt electronic environmental by the interaction metal-substrate. The Pt-TiO₂-C materials presented an increase in current density during oxide film formation on the surface of metallic particles at 0.8 V (NHE) (anodic sweep) compared with other catalysts prepared (M2-M4). Therefore a high current density of Pt oxide film reduction is observed centered at 0.75 V (NHE). This means a synergy activity formed between Pt nanocatalyst and TiO₂-C composites. For understand the Pt-TiO₂-C behavior, in the Fig. 4 right is presented the CO oxidation curves obtained from the CO stripping technique. Table 1, summarizes the electrochemical active area

EAS_{CO} obtained under the oxidation CO curve. The higher EAS_{CO} was observed in the 10%Pt-5%TiO₂-C electrocatalysts compare with the 10%Pt-5%SnO₂-C, 10%Pt-5%ZnO-C and 10%Pt-C materials prepared with the same methodology. The position of the maximum CO oxidation peak is similar for the four materials 0.77 V (NHE) (see Table 2).

3.5 Electrocatalytic Activity for the ORR

Fig. 5-a displays the ORR activity of Pt-oxide-C compared with Pt-C prepared by chemical vapor deposition method in oxygen saturated 0.5 M H₂SO₄ at a rotating speed of 900 rpm at 25°C. As observed the Pt-TiO₂-C electrocatalysts shows a shift in the EDR curves toward positive electrode potentials compared with the Pt/C, Pt-SnO₂-C and Pt-ZnO-C prepared by chemical vapor deposition.

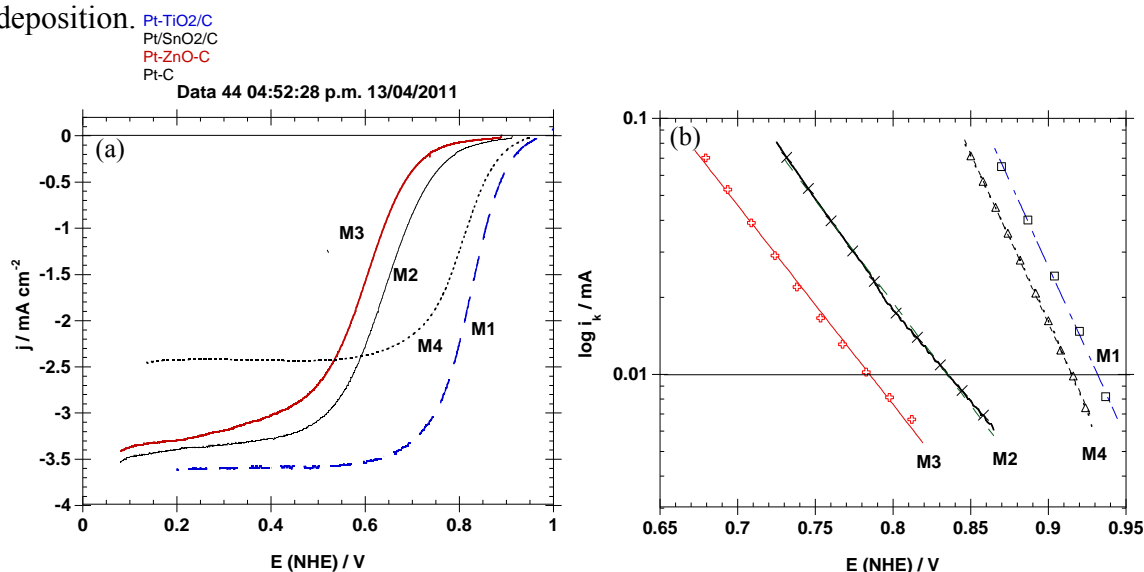


Figure 5. (a) ORR in saturated oxygen-electrolyte at 900 rpm in H₂SO₄ 0.5 M at 5 mV s⁻¹ and (b) Tafel slope on (M1)10%Pt-5%TiO₂-C, (M2)10%Pt-5%SnO₂-C, (M3)10%Pt-5%ZnO-C and (M4)10%Pt-C catalysts prepared by CVD.

Table 2 summarize the kinetic parameters deduced for the ORR on the Pt-TiO₂-C and Pt-C electrocatalysts in 0.5 M H₂SO₄ at 25°C (slope Tafel (mV dec⁻¹), Koutecky-Levich slope (mA⁻¹ rpm^{1/2}) and $E(NHE) / V$ a $j_k=0.01$ mA cm⁻²). The interaction of Pt with the TiO₂-C substrate shows an ORR kinetic current enhancement of 93 mA cm⁻² compared with Pt-C (0.91 mA cm⁻²).

In the case of the catalysts Pt-SnO₂-C and Pt-ZnO-C prepared by the same methodology, these materials present a lower electrochemical activity than Pt-C sample. This effect may be attributed at low interaction Pt-SnO₂ and Pt-ZnO obtained by this synthesis methodology. However, is necessary to obtained the TEM results of these samples (M2 and M3) for a complete analysis of their electrochemical behavior.

Table 2. Electrochemical parameters and electrochemical active surface of Pt-C and Pt-TiO₂-C electrocatalysts prepared by CVD

Catalysts	E (NHE) / V CO oxidation	-b, (mV dec ⁻¹)	Koutecky- Levich slope (mA ⁻¹ rpm ^{1/2})	E (NHE) / V a j _k =0.01 mA cm ⁻²
10%Pt-5%TiO₂-C	0.77	75	11.2	0.93
10%Pt-5%SnO₂-C	0.78	120	11.6	0.83
10%Pt-5%ZnO-C	0.77	122	7.6	0.78
10%Pt-C	0.77	75	9.8	0.91

Fig. 5-b shows the Pt-TiO₂-C and Pt-C samples present Tafel slopes. Table 2 summarizes the Tafel plot values of Pt-TiO₂-C and Pt-C around -0.75 V(NHE) dec⁻¹ and the Pt-SnO₂-C and Pt-ZnO-C presentes a around slope value of -0.120V(NHE) dec⁻¹. These different values depends of the energy of the oxygen adsorption and means that the transfer of the first electron to the O₂(ads) molecule is the determined step of the kinetic reaction. All samples prepared in this study show a similar Koutecky-Levich (K-L) slopes near of the theoretical value (9.8 mA⁻¹ rpm^{1/2}) were obtained. Pt-TiO₂-C, Pt-SnO₂-C and Pt presented a high K-L slope of 11.2, 11.6 and 9.8 mA⁻¹ rpm^{1/2} compare with Pt-ZnO-C (7.6 mA⁻¹ rpm^{1/2}). The ORR on the samples Pt-TiO₂-C, Pt-ZnO-C, Pt-SnO₂-C and Pt-C prepared by CVD is carried out preferentially the four electrons to the water formation.

4. CONCLUSIONS

Platinum nanoparticles deposited on TiO₂-C, SnO₂-C and ZnO nanocomposites as supports were prepared by chemical vapor deposition method. Their electrochemical activity in the ORR reaction was compared with Pt-C catalyst prepared by the same methodology. The Pt-C and Pt-oxide-C samples present a small particles size (< 3nm) with a homogeneous dispersion onto the substrate. The Pt-TiO₂-C showed an enhancement on their electrochatalytic activity for the ORR compared to conventional Pt-C catalyst due to TiO₂ presence. The Pt-Ti interaction promotes a ligand effect on the platinum electronic properties that increase the oxygen reduction and modified the platinum surface for the type of adsorption-desorption of hydrogen and carbon monoxide.

5. REFERENCES

- [1] J. Stumper, C. Stone, *J. Power Sources*, **176**, 468-476 (2008).
- [2] R.K. Ahluwalia, X. Wang, *J. Power Sources*, **177**, 167–176 (2008).
- [3] J. Larminie, A. Dicks, *Fuel Cell Systems Explained*, John Wiley & Sons Inc., West Sussex, England (2003).
- [4] P. Costamagna, S. Srinivasan, *J. Power Sources*, **102**, 242-252 (2002).
- [5] J. Chen, B. Lim, E. P. Lee, Y. Xia, *Nano Today* **4**, 81-95(2009).
- [6] B. Lim, X. Lu, M. Jiang, P.H.C. Camargo, E Chul Cho, E.P.Lee, Y. Xia, *Nano Lett.*, **8**, 4043-4047(2008).
- [7] H. Kangasniemi, D.A. Condit, T.D. Jarvi, *J. Electrochem. Soc.* **151**, 125-135 (2004).
- [8] M. Roen, C.H. Paik, T.D. Jarvi, *J. Electrochem. Solid-State Lett.* **7**, 19-22 (2004).
- [9] W.Vogel, L.Timperman, N. Alonso-Vante, *Appli. Catal. A* **377**, 167-173 (2010).
- [10] L. Timperman, Y.J. Feng, W. Vogel, N. Alonso-Vante, *Electrochim. Acta* **55**, 7558-7563 (2010).
- [11] J. Shim, C. Lee, H. Lee, J. Lee, E.J. Cairns, *J. Power Sources* **102**, 172-177(2001).
- [12] L. Xiong, A. Manthiram, *Electrochim. Acta* **49**, 4163-4170 (2004).

- [13] N. Rajalakshmi, N. Lakshmi, K.S. Dhathathreyan, *Int. J. Hydrogen. Energy* **33**, 7521-7526 (2008).
- [14] S.v. Kraemer, K. Wikander, G. Lindbergh, A. Lundblad, A.E. Palmqvist, *J. Power Sources* **180**, 185-190 (2008).
- [15] M. Gustavsson, P. Ekström Hanarp., L. Eurenus, G. Lindbergh, E. Olsson, B. Kasemo, J. *Power Sources* **163**, 671-678(2007).
- [16] K. Sasaki, L. Zhang, R. R. Adzic, *PCCP* **10**, 159-167 (2008).
- [17] K.-W. Park, K.-S. Seol, *Electrochem. Commun.* **9**, 2256-2260 (2007).
- [18] N.R. Elezovic, B.M. Babic, V.R. Radmilovic, L.M. Vracar, N.V. Krstajic, *Electrochim. Acta* **54**, 2404-2409 (2009).
- [19] X.-Y.Xie, Z.-F. Ma, X. Wu, Q.-Z. Ren, X. Yuan, Q.-Z. Jiang, L. Hu, *Electrochim. Acta* **52**, 2091-2096 (2007).
- [20] V. Mentus Slavko, *Electrochim. Acta* **50**, 3609-3615 (2005).
- [21] N.R.Tacconi, C.R. Chenthamarakshan, K. Rajeshwar, W.Y. Lin, T.F. Carlson, L. Nikiel, W.A. Wampler, S. Sambandam, V. Ramani, *J. Electrochem. Soc.* **155**, 1102-1109 (2008).
- [22] L. Timperman, A. Lewera, W. Vogel, N. Alonso-Vante, *Electrohem. Comm.* **12**, 1772-1775 (2010).
- [23] B. Ruiz-Camacho, M. A. Valenzuela, J. A. Pérez-Galindo, F. Pola, M. Miki-Yoshida, N. Alonso-Vante, R. G. González-Huerta, *J. New Mat. Electrochem. Syst.*, **13**, 183-189 (2010).
- [24] M. Harada and H. Einaga, *Langmuir* **22**, 2371-2377 (2006).
- [25] T. Vidakovic, M. Christov, D. Sundmacher, *Electrochim. Acta* **52**, 5606-5613(2007).